Polyelectrolyte Microstructure in Chitosan Aqueous and Alcohol Solutions

N. Boucard,[†] L. David,*[,†] C. Rochas,[‡] A. Montembault,[†] C. Viton,[†] and A. Domard[†]

Laboratoire des Matériaux Polymères et des Biomatériaux, Université de Lyon, Université Lyon 1, UMR CNRS 5223 IMP, 15, Bd. A. Latarjet, Bât. ISTIL, 69622 Villeurbanne Cédex, France, and Laboratoire de Spectrométrie Physique, Université Joseph Fourier, UMR CNRS 5588, 140 Avenue de la Physique, B.P. 87, 38402 Saint Martin d'Hères Cédex, France

Received September 24, 2006; Revised Manuscript Received January 12, 2007

This work deals with chain ordering in aqueous and water−alcohol solutions of chitosan. The so-called polyelectrolyte peak is investigated by small-angle synchrotron X-ray scattering. The polyelectrolyte microstructure was characterized by the position of the maximum of the polyelectrolyte scattering peak q_{max}, which scales with the polymer concentration c_p as $q_{max} \sim c_p^{\alpha}$. An evolution of the power law exponent α is observed as a function of the degree of acetylation (DA) of chitosan, which is responsible for changes of both the charge density (f) and the hydrophobicity of the polymer chains. The results highlighted the two organization regimes of the theory of Dobrynin and Rubinstein,[1] investigated here for the first time for a natural polymer. At low DAs, $\alpha \approx 1/2$, in agreement with a pearl necklace organization where the structure is controlled by the string between pearls. For higher DA, $\alpha \approx 1/3$, and the correlation revealed by the polyelectrolyte peak is controlled by the pearls. This analysis offers a way to study quantitatively the balance between solvophobic−solvophilic interactions that play an important role in the solution properties of natural polymers. In addition, the role of several parameters acting on the interaction balance were evidenced, such as the nature of the counterion, the composition of the solvent (amount of alcohol in the aqueous solution), and the screening of Coulombic forces by salt addition. Finally, the nanostructure transition from a polyelectrolyte solution to a physical gel is discussed. The gel state is reached when the solvophobic interactions are favored, but depending on the gelation route the polyelectrolyte ordering could be preserved or not.

Introduction

Polyelectrolytes are particularly attractive for their great interest in various fields of applications including molecular biology,[2] partly since numerous biological macromolecules are polyelectrolytes such as RNA, DNA,[3,4] cationic or anionic polysaccharides (chitosan,[5] carrageenan,[6] hyaluronan[7]), or proteins (actin,[8] albumin, γ-globulin). Synthetic polyelectrolytes have also been extensively studied, especially polystyrene sulfonate (PSS), which we can consider as the reference synthetic system. The properties of polyelectrolyte solutions are based on complex multi-scale interaction mechanisms involving the primary structure of the polyions, counterions, co-ions, and solvent.

The theory of polyelectrolyte solutions was investigated experimentally and theoretically in a large number of studies, reviewed by Barrat and Joanny.[9] The difficulty in capturing a precise picture and a molecular origin of the polyelectrolyte conformation and ordering in solution is due to the different length scales involved in the description of interacting charged chains. At the local scale, the first degree of complexity is related to the ability of a fraction of counterions to form a charged layer (ionic condensation) closely interacting with the polymer chains.[10,11] Condensation decreases the effective charge carried by the macro-ion and is believed to induce long-range effects since fluctuations in the charged clouds around the polymer chains create electrostatic attractions between macromolecules similar to van der Waals attractions between electronic clouds of molecules.

At a higher observation scale, the chain conformation is described as corresponding to a succession of segments or subunits or electrostatic blobs.[12] In dilute salt-free solutions, therefore, the polymer conformation corresponds to an extended chain of electrostatic blobs resulting from repulsion between blobs. At higher polymer concentrations, the succession of electrostatic blobs adopts the dilute regime conformation over distances shorter than the correlation length ξ, which also corresponds to the distance between chains. For length scales greater than ξ, the chain is governed by Gaussian statistics.[13,14] The scaling description for the case of solvophobic polyelectrolytes was further developed, leading to the pearl necklace model.[1] The conformation of a polymer chain at low charge density is that of a globule, but if the charged monomer fraction f increases, this globule splits into smaller hydrophobic beads (pearls) connected by extended portions of electrostatic blobs (strings). Experimentally, the structure of a polyelectrolyte solution is revealed by the presence of a correlation polyelectrolyte peak in the neutron,[7,15−20] light,[3,4,19] or X-ray small-angle scattering curves.[6,21−23] The position of this peak at q_{max} reflects the value of the interchain or correlation distance since

$$\xi \approx 2\pi/q_{max} \tag{1}$$

The value of ξ and its relationship with q_{max} were originally verified by atomic force microscopy.[24,25]

In good solvents, the scaling law of q_{max}, and hence ξ with the polymer concentration c_p, is known to be different in the

* Corresponding author. E-mail: Laurent.David@univ-lyon1.fr.
[†] Université de Lyon.
[‡] Université Joseph Fourier.

10.1021/bm060911m CCC: $37.00 © 2007 American Chemical Society
Published on Web 03/09/2007

case of the dilute ($c_p < c_p^*$, where $q_{max} \sim c_p^{1/3}$) and semidilute regimes ($c_p > c_p^*$ where $q_{max} \sim c_p^{1/2}$). For solvophobic polyelectrolytes,[1] the scaling is more complicated in the semidilute regime since there exists a crossover concentration c_b between the string-controlled regime ($c_p < c_b$ where $q_{max} \sim c_p^{1/2}$) and the solvophobic bead-controlled regime ($c_p > c_b$ where $q_{max} \sim c_p^{1/3}$). The scaling law exponents were verified in many studies in good solvent, and less extensively in the case of poor solvents.[18,22,25,26] Numerical simulation techniques[27−30] are also tools for the understanding of the structure of polyelectrolyte solutions, but a review of the various simulation techniques and predictions is out of the scope of the present paper.

At a third level of organization, a polyelectrolyte correlation coexists with chain aggregation domains.[31] The size of these domains is much larger than the correlation distances, and thus, small-angle X-ray elastic scattering intensities in the small q range exhibit an increase of the form $I(q) = C/q^4$,[7,19] although other authors find different scattering laws.[4,5,15] Addition of salt to the solution produces an increase in the low-angle scattering contribution of the large-scale structures. Dynamic light scattering classically exhibits two optical relaxation modes, the slowest being related to the diffusion of polyelectrolyte domains.[4,19] Finally, the existence of liquid−crystal phases in the semidilute regime has been observed, and in the dilute regime, a transition in chain ordering from crystalline to gas phases was predicted for vinyl-type polyelectrolyte solutions.[32]

Chitosan is commonly obtained from the chemical N-deacetylation of chitin, one of the two most widespread natural polymers with cellulose.[33] Chitin and chitosan belong to the same series of linear copolymers of *N*-acetyl-D-glucosamine and d-glucosamine with $\beta(1 \rightarrow 4)$ glycosidic linkages. When the distribution of the two constitutive residues is random, chitosan corresponds to a degree of acetylation (DA) (i.e., the molar fraction of *N*-acetyl-D-glucosamine residues) below 70%. This limit is related to the value below which it is always possible to dissolve the polymer in dilute acidic solution at pH < 6, well below the intrinsic pK (pK_o) of the NH_3^+ moieties. Chitosan can also be obtained in other physical forms such as chemical and physical hydrogels,[34−37] films,[38] nanoparticles,[39] and fibers.[40] The whole series of copolymers has been extensively studied in pharmaceutical and medical fields for its biodegradability, biocompatibility, bioactivity, and physicochemical properties.[41]

As a result of a chemical structure bearing both ionic and hydrophobic sites, the physical, physicochemical, and biological properties of chitosan are known to depend on structural parameters such as the DA and the distribution of the two kinds of repeating units along the chains.[33] These properties are also influenced by external parameters including pH, ionic strength, dissociation degree of the amine groups present on the *N*-acetyl-D-glucosamine residues,[42−44] dielectric constant of the medium, and temperature.[35]

Among the analytical techniques allowing the investigation on the chitosan solution behavior, viscosimetry[33,45−47] and static light scattering[43,48−50] are the most commonly used. Although the studies on physicochemical properties and conformations of chitosan in aqueous solution at high ionic strength are numerous, most of these only reported analyses on a restricted range of chitosan in terms of DA.[46,51−53] Commercial samples were generally used without further purification and degraded by means of sonification,[54] nitrous deamination,[55] or acidic hydrolysis, leading to relatively high and variable polydispersity indexes[49] (I_P). Such values of I_P necessarily do not allow a careful study of solution properties. Furthermore, the distribution of the GLcN and GlcNAc residues along the polymer chain can exhibit composition heterogeneities[45,56] that also represent a drawback for the study of behavior in aqueous solutions. Recently, the existence of general trends in the behavior for chitosan in aqueous solution as a function of DA was revealed on homogeneous series of copolymers with similar and low I_p values by Sorlier et al.,[57] Schatz et al.,[43] and Lamarque et al.[44].

Our aim was to gain insight into the molecular organization and conformation of chitosan in solution with the polymer concentration c_p ranging from 2 g/L up to 30 g/mL (i.e., above the critical chain entanglement concentration c_p^* in the semidilute regime). The structural length b of the repeat unit is about 5.1 Å for both *N*-acetyl-D-glucosamine and d-glucosamine residues. For a statistical copolymer of charged and uncharged repeat units, the average distance between two charges is given by $b/(1 - DA)$. Indeed, the amino sites can be considered as fully ionized at a pH near 4.5. Thus, assuming the interaction parameter u as the ration between the Bjerrum length l_B (7.2 Å in water at 25 °C) and the average distance between two charges

$$u = (1 - DA)l_B/b \qquad (2)$$

ion condensation[10,11] should occur for $u > 1$ (i.e., for acetylation degrees DA below 28%), the effective charged fraction of repeating units is about 70%, and the maximum fraction of counterions involved in the condensation is close to 30%. Evidence for this ionic condensation threshold was clearly shown in previous papers[43,44,57] by considering the variation of various physicochemical parameters of chitosan solutions with DA.

We measured the intrinsic viscosity (η_o) in an acetic acid−ammonium acetate buffer solution (0.2 M/0.5 M) at pH = 4.5 and defined a characteristic concentration c^* as the inverse of (η_o).[58] Depending on the sample studied, $c^* \cong 0.01-0.04\%$ (w/w) (i.e., $c^* \cong 0.1-0.4$ g/L). These values are necessarily higher than the concentration c_p^* in salt-free solutions, but they imply that for all the solutions of chitosan presented next, the polymer concentration significantly exceeded c^* and was thus greater than c_p^*.

In this paper, a detailed study of the polyelectrolyte ordering of chitosan solutions with controlled molecular structure (low I_P, high molecular weight, true statistical distribution of residues) is reported. Chitosan is then considered as a model hydrophobic polyelectrolyte system where the scaling of the polyelectrolyte peak location with the polymer concentration was studied by synchrotron SAXS as a function of the charge density, nature of the counterion, salt addition, solvent composition, and sol−gel transition.

Experimental Procedures

Purification of Chitosan. We used two batches of chitosan produced from squid pens, purchased by Mahtani Chitosan. The first (no. 114) had an initial DA of 5.2%, and the second (no. 114 15/11/02), 2.6%. For purification, chitosan was dissolved at 0.5% (w/w) in acetic acid to obtain the stoichiometric protonation of the NH_2 sites. The mixture was filtered successively through 3, 1.2, 0.8, and 0.45 μm Millipore membranes. The polymer was then precipitated using aqueous ammonia (28% (w/w)). After several washing and centrifugation steps in deionized and distilled water, until a neutral pH was achieved, the precipitate was lyophilized.

Table 1. Degree of Acetylation (DA), Water Content, Degree of Polymerization by Weight (DP_w), Polydispersity Index (I_p), and Weight-Average Number of Charged Segments/Chain of the Different Samples of Chitosan Prepared and Investigated in this Work

DA (%)	water content (% (w/w))	DP_w	$I_p = DP_w/DP_n$	wt-av no. of charged segments/chain
2.6[a] ± 0.1	8.0 ± 0.9	2082 ± 105	1.6 ± 0.2	2028
5.2 ± 0.3	7.4 ± 0.7	1543 ± 103	2.1 ± 0.2	1463
10.7[a] ± 0.4	7.25 ± 0.6	1477 ± 99	1.8 ± 0.2	1319
20.2[b] ± 0.5	8.7 ± 0.9	1504 ± 97	2.0 ± 0.2	1200
30.2[a] ± 0.2	8.04 ± 0.8	1551 ± 98	1.8 ± 0.2	1083
36.7[b] ± 1.8	9.6 ± 1.0	1467 ± 98	1.8 ± 0.2	929
46.2[b] ± 2.3	11.5 ± 1.2	1359 ± 99	2.1 ± 0.2	731
52.1[b] ± 0.9	9.36 ± 1.2	1501 ± 99	2.0 ± 0.2	719
65.5[b] ± 3.3	12.4 ± 1.2	1312 ± 99	1.9 ± 0.2	453

[a] Samples obtained from the raw material of DA = 2.6%. [b] Samples obtained from the raw material having DA = 5.2%.

Acetylation of Chitosan. From the two batches mentioned previously, samples of different DA where prepared by re-acetylation. The N-acetylation of chitosan was obtained in a water−1,2-propanediol mixture with acetic anhydride as the reagent.[59] Thus, chitosan was dissolved in distilled and deionized water containing the amount of acetic acid necessary to achieve the stoechiometric protonation of the NH_2 sites. Then, 1,2-propanediol was added to achieve a final polymer concentration of 0.5% (w/w), with equal amounts of water and alcohol (50%/50% (w/w)). A solution of pure and fresh acetic anhydride in 1,2-propanediol, whose composition was the stoechiometric ratio anhydride−glucosamine necessary to prepare the required DA, was slowly added under strong stirring. The medium was left to stand for 3 h. The obtained chitosan was precipitated with aqueous ammonia (28% (w/w)). The polymer was washed in deionized and distilled water and lyophilized as described previously. The structural characteristics and water content of all the samples prepared and studied in this work are listed in Table 1.

Determination of DA. The DA of the different samples was deduced from ^1H NMR spectroscopy. Spectra were recorded on a Brucker 250 spectrometer (250 MHz) at 25 °C. A total of 10 mg of chitosan was dissolved in 1 g of D_2O, in presence of HCl. The DA was calculated using the method developed by Hirai et al.,[60] from the ratio of the area of the methyl protons of the *N*-acetylglucosamine residues to that of the H_2 to H_6 protons of both glucosamine and *N*-acetyl glucosamine residues.

Determination of M_w. The weight-average molecular weight M_w was evaluated by size exclusion chromatography (SEC). SEC was performed with an IsoChrom LC pump (Spectra-Physics) connected to a Protein Pack glass 200 SW column and a TSK 6000PW gel. A Waters 410 differential refractometer and a multi-angle laser-light scattering detector (632.8 nm; Wyatt Dawn DSP) were connected online. A 0.15 M ammonium acetate/0.2 M acetic acid buffer (pH 4.5) was used as an eluent. Chitosan was dissolved in the buffer (1 mg/mL), filtered on a 0.45 μm Millipore membrane, and then injected (100 μL). The refractive index increment (at 632.8 nm) depending on the DA was taken from previous results.[43]

Determination of the Initial Water Content. The water content was evaluated using a thermogravimetric analyzer, DuPont Instrument 2950. About 10 mg of chitosan was analyzed under helium flow, operating at a temperature ramp of 2 °C/min from 30 to 150 °C. The concentration of chitosan solutions could be thus evaluated, taking into account the initial water content of chitosan representing about 8% of the of solid mass.

Preparation of Solutions. Chitosan was dispersed in water and pure acetic acid, or an aqueous solution of hydrochloric acid (37% (w/w) (in water)) was added to achieve the stoechiometric protonation of the NH_2 sites. The mixture was stirred overnight. For the study in the hydro-alcoholic medium, 1,2-propanediol was added (50% (w/w)) to the previous solution, and the mixture was stirred for 1 h.

Synchrotron SAXS. Small-angle X-ray scattering was performed on the BM2-D2AM beamline at the ESRF (Grenoble, France). A synchrotron source was required for our study since the intensity scattered by the polyelectrolyte solutions was not accessible by conventional sources in point collimation conditions. The data were collected at an incident photon energy of 16 keV. We used a two-dimensional detector (CCD camera from Ropper Scientific). All the data corrections were performed with the bm2img software available on the beamline. The data were corrected for dark current, flat field response, and taper distortion. Finally, the azimuthal average around the image center (position of the center of the incident beam) was performed for the *q*-range calibration standard (silver behenate) and the chitosan solutions. The polyelectrolyte solutions were placed in low-density poly(ethylene) (LDPE) cylindrical sample holders (internal diameter of about 5 mm) with two kapton windows. The contribution of the cell filled with water or alcohol−water mixtures was subtracted from the scattering curves of the samples studied, after normalization by the transmitted intensity and the intensity decay of the beam.

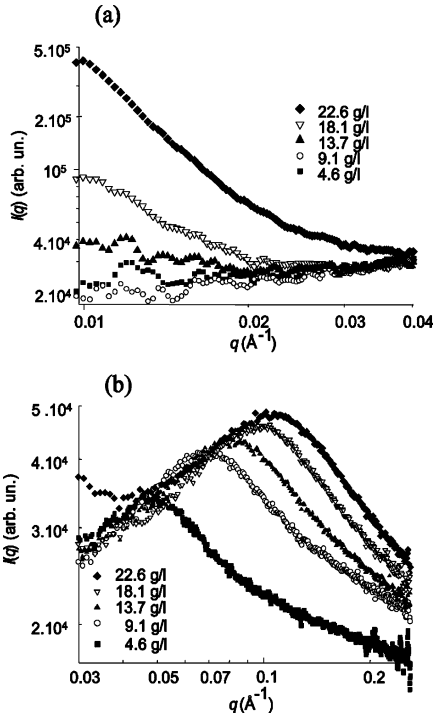

Figure 1. Log−log plot of the scattering curves for a chitosan acetate aqueous solution with DA = 10.7% and polymer concentrations ranging from 4.6 to 22.6 g/L (a) in the scattering vector range of the low-angle upturn. The amplitude of the low-angle upturn increases with polymer concentration (b) in the scattering vector range of the polyelectrolyte peak. The position and amplitude of the scattering peak are sensitive to polymer concentration.

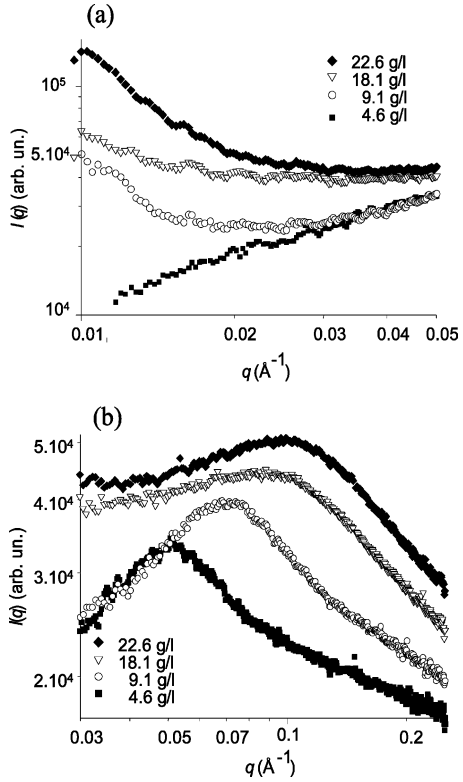

Figure 2. Log−log plot of the scattering curves for chitosan hydrochloride aqueous solution with DA = 10.7% and polymer concentrations ranging from 4.6 to 22.6 g/L (a) in the scattering vector range of the low-angle upturn. The amplitude of the low-angle upturn is sensitive to polymer concentration (b) in the scattering vector range of the polyelectrolyte peak.

Determination of q_{max} and the Shape of Scattering Curves. The shape of the scattering curves $I(q)$ was found from the relation

$$I(q) = D + \frac{C}{q^{\gamma}} + \frac{B}{1 + 4\left[\frac{q - q_{max}}{w}\right]^2} \qquad (3)$$

This equation is similar to that proposed by Wang.[15] The parameter γ improves the fit in the low q range. q_{max} represents the position of the maximum of the Lorentzian polyelectrolyte peak; w is the full width at half-height, and B is the intensity of the polyelectrolyte peak. D is a constant baseline parameter. This contribution is weak and could be neglected in many cases. The term C/q^{γ} takes into account the contribution of large-range electronic density fluctuations. The values of q_{max} deduced from eq 4 were in good agreement with a direct visual estimation of the position of the polyelectrolyte peaks on the scattering curves (the differences did not exceed 3×10^{-3} Å^{-1}).

Results and Discussion

Small-angle X-ray scattering diagrams of chitosan solutions corresponding to the acetate form in stoechiometric conditions are shown on Figure 1a,b for different polymer concentrations at a DA close to 10.7%. Figure 1a displays the low-angle range with the upturn contribution arising from aggregated chain domains, whereas Figure 1b shows the polyelectrolyte peaks observed at higher q values in the same conditions. In Figure 2 a,b are reported the corresponding results obtained from chitosan solutions with the same DA, in the hydrochloride form, still in stoechiometric conditions.

For both salts, the upturn at low angles is more apparent for the highest concentrations, although a fluctuation in the magnitude of this contribution to the scattering curves can be observed. This variability noted for the lowest concentrations studied is not due to aging of the solutions but could reflect heterogeneities in the aggregate size/content at the scale of the cross-section of the incident beam (i.e., about 100 μm × 300 μm). However, as a general rule, solutions at the highest concentrations (i.e., above 10 g/L) are heterogeneous and consist of a polyelectrolyte solution in which are embedded larger scale domains composed of aggregated chains. Such conclusions were also reached previously by dynamic light scattering of chitosan solutions with varying DA and concentrations.[61] From these light and X-ray scattering results alone, it is rather difficult to estimate the exact amount of polymer involved in both phases, which, however, should remain relatively low.

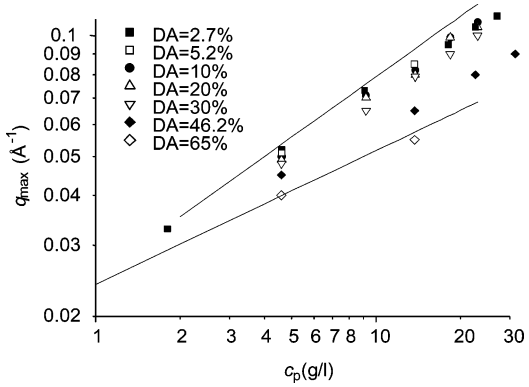

Figure 3. Scaling relation of the position of the polyelectrolyte peak q_{max} in chitosan acetate solutions as a function of the polymer concentration c_p for different degrees of acetylation, DA = 1 − f, where f is the charged monomer fraction. Solid lines with $(c_p)^{1/2}$ (upper curve) and $(c_p)^{1/3}$ (lower curve) dependence are guides for the eye.

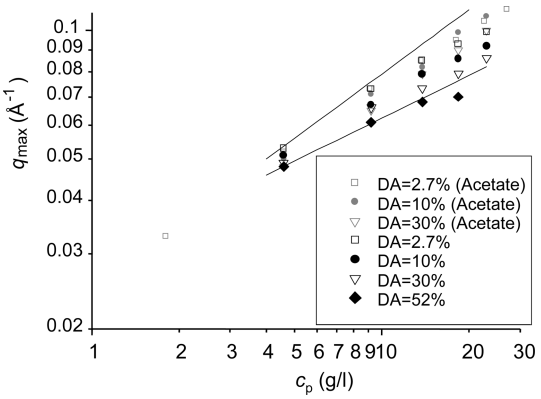

Figure 4. Scaling relation of the position of the polyelectrolyte peak position q_{max} in chitosan hydrochloride solutions as a function of the polymer concentration c_p, for different degrees of acetylation, DA = 1 − f, where f is the charged monomer fraction. Solid lines with $(c_p)^{1/2}$ (upper curve) and $(c_p)^{1/3}$ (lower curve) dependence are guides for the eye. The gray symbols (smaller) display comparable data from Figure 3 with the same DA and show that the value of q_{max} is sensitive to the counterion nature (acetate or choride anions).

The displacement of the polyelectrolyte peak toward higher values of q with increasing nominal polymer concentration is presented in Figure 3 for acetate counterions and a large range of DAs. Figure 4 displays similar results in the case of chloride counterions at several DA values.

The results obtained with chitosan acetate are similar to published data on polystyrene sulfonate[18] with different fractions f of ionizable units. In our case (see Figure 3), the value of DA is comparable to 1 − f, and a gradual decrease in the exponent of the law of variation of q_{max} with c_p from $\alpha = 1/2$ at low DA (high charge density) to $\alpha = 1/3$ at high DA (low charge

density) is observed for chitosan acetate. In the case of the hydrochloride form of chitosan, at the highest DA and c_p values, q_{max} scales with c_p with an exponent much lower than 1/3, also in good agreement with the results of Waigh et al.,[22] with a reported value close to 1/7. These results find a natural interpretation in the theory of Dobrynin and Rubinstein[1,62] for solvophobic polymers, in terms of a transition from a necklace-type model with a structure controlled by the organization of the strings between pearls ($\alpha = 1/2$) to a situation dominated by the hydrophobic pearls ($\alpha = 1/3$). These two situations correspond to the string- and bead-controlled regimes. Chitosan can thus be seen as a hydrophobic polymer in water, as in the case of hyaluronan[7] (although no polyelectrolyte peak could be detected in the latter case). Moreover, the predictions of Dobrynin and Rubinstein[1] are in striking agreement with experimental data (see the comparison between experimental results[22] and theoretical predictions[1,62]), with the identification of several organization regimes as a function of the concentration. In this study, only two regimes are identified since homogeneous solutions at $c_p > 40$ g/L could not be obtained. The crossover concentration between these two regimes, c_b, is related to the charge density parameter f and the solvent quality (or the solvophobicity) parameter $\tau = (\theta - T)/\theta$, where θ is the θ temperature, through[1]

$$c_b = \frac{1}{b^3}\left[\frac{uf^2}{\tau}\right] \quad (4)$$

The increase of the acetylation degree DA is responsible for an increase of the parameter τ and a decrease of f when the value of DA is above the Manning condensation threshold.

Our results do not allow a precise calculation of the value of c_b as a function of DA, but this value is slightly lower than 10 g/L (Figure 4) for the lowest DA in the acetate and hydrochloride forms of the chitosans studied, while c_b decreases below 4 g/L for the highest DA, as a result of the decrease of f and a concomitant increase of the solvophobicity parameter τ. The role of the latter parameters was previously illustrated on considering the gelation mechanism as a function of DA.[35] Thus, the water content on the gel point was found to increase continuously with DA up to DA $\approx$ 45%.

The existence of a critical polymer concentration c^{**} in the semidilute regime was previously observed after the study of various physicochemical parameters as a function of the chitosan concentration. Indeed, the changes with c_p of the zero-shear viscosity,[36] the pH at the gel point,[36] the time to reach the gel point,[36] and the equilibrium storage modulus of the gels[36] allowed us to define a change of behavior at a critical concentration that also defines a limit between two structural organization regimes in chitosan solution.[36] We thus identify c^{**} as the limit between the string-controlled and the bead-controlled regimes c_b. We also confirmed this behavior in a recent study of the kinetics of gelation of chitosan solutions both with the acetate and hydrochloride forms of chitosan.[37]

Concerning our data, the observed behavior at DA < 25%, where Manning−Osawa ionic condensation is expected, cannot be explained by the change in f alone since f should be constant and comparable to $f_{eff} \sim b/l_B$. Indeed, in the case of hydrophilic polyelectrolytes, charge renormalization occurs, and the position of the polyelectrolyte peak is independent of f in the condensation regime.[17,18] In the case of hydrophobic polymers, the dependence upon c_p of q_{max} at low DA in the domain where α is close to 1/2 (in the string-controlled regime) should reflect the variation of τ at constant $f = f_{eff}$ according[62] to

$$q_{max} \approx b^{-1}\left[\frac{f^2 l_B}{b\tau}\right]^{1/4}(c_p b^3)^{1/2} = q_0(c_p,\tau,b)f^{1/2} \quad (5)$$

This results[62] in a slight decrease of q_{max} in the log−log plots of $q_{max}(c_p)$ with increasing DA as observed in Figures 3 and 4 (i.e., a reduction[22] in the gradient of $q_{max}/c_p^{1/2}$). For larger DA values, above 40%, the bead-controlled regime is modeled by[62]

$$q_{max} \approx b^{-1}\left[\frac{f^2 l_B}{b\tau}\right]^{1/3}(c_p b^3)^{1/3} = q'_0(c_p,\tau,b)f^{2/3} \quad (6)$$

Eq 5 is consistent with the experimental data only for large DA values. This is illustrated in Figure 5, which shows the variation of q_{max} with DA at a constant value of c_p close to 13.8 g/L.

In this figure, the effect of the nature of the counterion is most pronounced at low DA. In this range, the height of the curve corresponding to the hydrochloride form of the chitosan polyelectrolyte peak is systematically lower than that of the chitosan acetate. By contrast, in the high DA range (over 50%), where the counterion concentration and polymer charged fraction f are weak, the behavior becomes independent of the nature of the counterion. This suggests that the chitosan hydrochloride is a more hydrophobic polyelectrolyte than chitosan acetate in the condensation regime, so that the solvophobicity parameter τ should characterize specifically the polyelectrolyte−counterion−solvent interactions. As shown by molecular modeling,[63] in terms of molecular associations, acetate ions can interact with glucosamine residues by a combination of electrostatic and hydrogen bonding through the formation of a complex involving both the amine site and the OH group on carbon 3. The hydrochloride form corresponds to the formation of simple ion pairs that do not enhance the solubility of the polymer in water. Indeed, hydrogen bonding cannot involve chloride anions, and the polymer in the same solvent is in a slightly more hydrophobic environment when inorganic anions are present. In the intermediate DA range, the slope of the q_{max} versus DA curve gradually decreases with decreasing DA, as a result of various contributions, namely: (i) the transition from bead-controlled to string-controlled regime (i.e., a change from $f^{2/3}$ (eq 6) to $f^{1/2}$ (eq 5) scaling laws[62]), (ii) a decrease of τ with decreasing the *N*-acetyl glucosamine residue fraction, and (iii) ionic condensation inducing a more or less constant effective value of the parameter f.

The results displayed in Figures 3−5 provide fresh arguments in favor of a general behavior of chitosan solutions that was previously described on studying the variation of chitosan solution properties (dn/dc,[43] Mark−Houwink−Khun−Sakurada equation parameters[44]) as a function of DA.[36,43,44,57] This law is characterized by three domains of behavior as a function of DA. Below 25%, standard polyelectrolyte behavior is found with an upper limit defined by the Manning theory of ionic condensation. For DA > 50%, chitosan behaves like a hydrophobic polymer with a low charge fraction, while an intermediate range occurs corresponding to a transition between the two regimes in which the physiochemical properties vary weakly with DA.

Role of the Solvent. The role of the solvent was studied by comparing the polyelectrolyte peaks observed in water and in a mixture of water and 1,2-propanediol (50% (w/w)). Figure 6 shows the role of the addition of the alcohol in the aqueous medium on the polyelectrolyte peak of chitosan with DA = 2.7%, in the case of acetate counterions. Figure 7 displays similar results in the case of chloride counterions.

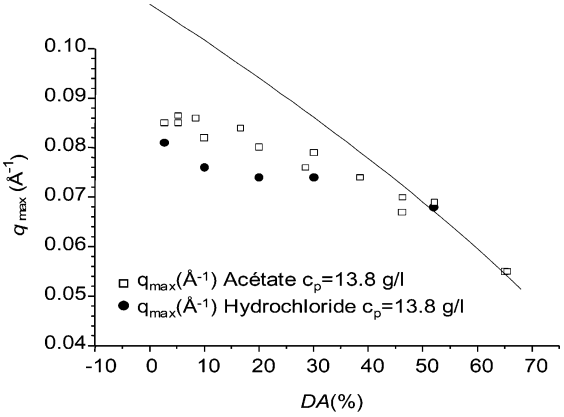

Figure 5. Evolution of the maximum of the polyelectrolyte peak q_{max} as a function of DA at fixed concentration 13.8 g/L for chitosan hydrochloride and acetate solutions. The solid line is the $f^{2/3}$ prediction of eq 6 (see text).

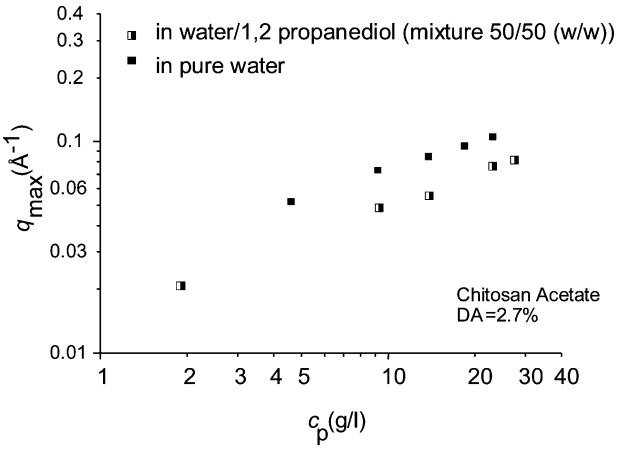

Figure 6. Concentration dependence of the maximum of the polyelectrolyte peak q_{max} in two solvents (water and 1,2-propanediol−water 50:50 (w/w)) in chitosan acetate solutions, DA = 2.7%.

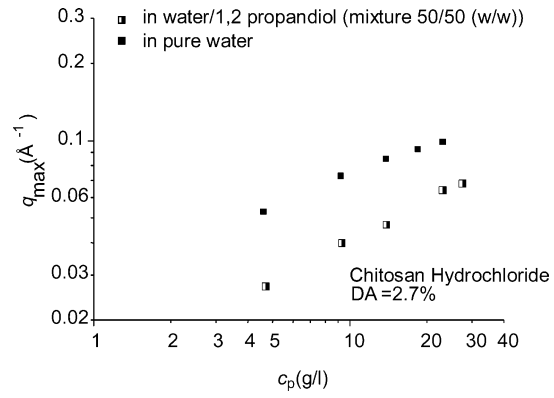

Figure 7. Concentration dependence of the maximum of the polyelectrolyte peak q_{max} in two solvents (water and 1,2-propanediol−water 50:50 (w/w)) in chitosan hydrochloride solutions, DA = 2.7%.

At this value of DA, the $c_p^{1/2}$ scaling law is observed in water (as previously shown in Figures 3 and 4) and is preserved in the case of the mixed alcohol−water solvent. Nevertheless, the values of the position of the maximum of the polyelectrolyte peak decrease in the presence of alcohol. Again, this result should be interpreted as a change in the factor $[f^2 l_B/b\tau]$ in eq 6. The change in l_B should reflect that of the relative dielectric constant, which is much higher in water (close to 80) than in propandiol (close to 27.5). As a result, the Bjerrum length at 25 °C increases from 7.2 Å to about 10 Å, assuming that the dielectric constant is the average of that of the two solvents. If

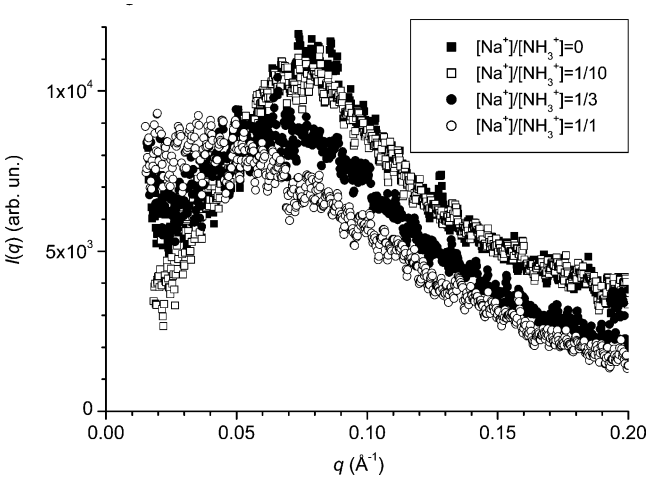

Figure 8. Dependence on added NaCl of the polyelectrolyte peak in a chitosan hydrochloride solution with DA = 2.7% and concentration c_p = 9.1 g/L, where the molar concentration ratio of cations is r_s = [Na$^+$]/[NH$_3^+$]. q_{max} decreases with increasing added salt.

we use the ionic condensation regime predictions, this in turn decreases the effective charge fraction $f_{eff} = b/l_B$ from 70% in water to 50% in water−alcohol mixtures. The change in the factor $f^2 l_B$ is in good agreement with the difference in the data shown in Figure 6. We conclude that in the case of acetate counterions, the evolution of the solvophobicity parameter τ is weak, and the shift in the position of the polyelectrolyte peak is due mainly to the change of the charge fraction f_{eff}. In the case of chloride counterions, the polymer is more solvophobic, and the observed difference between the $q_{max}(c_p)$ plots in water and the $q_{max}(c_p)$ plots in the alcohol−water mixtures is greater. This cannot be attributed to the change of $f^2 l_B$ alone. It is thus concluded that the decrease of τ plays a more important role in the evolution of q_{max} when chloride counterions are present.

It is difficult to describe more quantitatively the variation of the parameters involved in the Dobrynin equation since ion condensation in solvophobic polymers is more complex than in solvophilic conditions.[1] The expressions for the effective charge fraction, however, are strictly valid in this case.

Role of Added Salt. We also investigated the role of the ionic strength by adding salts of monovalent ions at different concentrations c_s. In some earlier works in the literature, there was disagreement about the role of the ionic strength in polyelectrolyte solutions. Some authors found that the addition of a small amount of salt induced a shift of q_{max} toward lower q values,[64,65] while others observed no influence of the concentration of the added salt on the position of the polyelectrolyte peak.[3,4] In all cases, however, a decrease in the magnitude of the polyelectrolyte peak was observed with increasing salt concentration.[20] In the context of this paper, the influence of the added salt is expected to be somewhat complex since it should depend on the nature of the counterions and on the added salt, particularly in the high polymer concentration range and/or in the low DA range, where the nature of the ions influences the solvophobicity of the polyelectrolyte.

In the low c_s range, the nature of the added ions has a weak effect. Figure 8 shows the influence of the molar concentration ratio r_s = (Na$^+$)/(NH$_3^+$) after the addition of sodium chloride in a solution of chitosan hydrochloride with c_p = 9.1 g/L and DA = 2.7%. The nature of the anions is thus kept constant. A clearly apparent shift in the position of the polyelectrolyte peak is observed with increasing added salt content.

According to Dobrynin and Rubinstein,[62] the shift of the polyelectrolyte peak is governed by the factor $(1 + 2c_s/c_p)^{-1/4}$

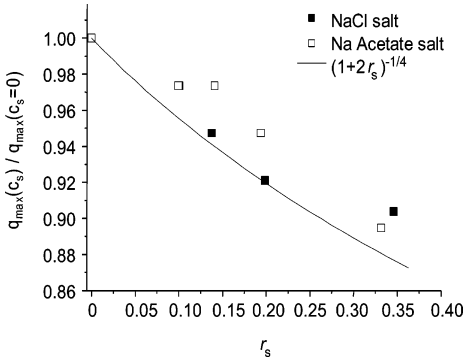

Figure 9. Variation of the polyelectrolyte peak in a chitosan hydrochloride solution with $r_s = [Na^+]/[NH_3^+]$. Solid line is the Dobrynin prediction for the string-controlled regime.

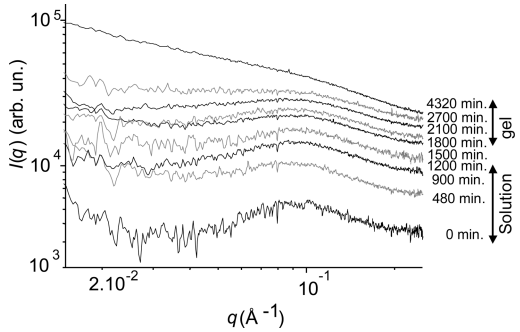

Figure 10. SAXS curves of chitosan hydrochloride (DA = 2.7%, c_p = 27 g/L) in a water−1,2-propanediol mixture as a function of evaporation time. Initial solution samples were disks of diameter 30 mm and thickness 10 mm. They were processed from an initial weight of solution of 6.00 g ± 0.02 g, at 50 °C. The gel was formed by the hydroalcoholic solvent route with an evaporation time of about 1200 min. At the gel point, water is almost completely removed, and 20% of the initial concentration of chloride ions remains. The polyelectrolyte peak is still visible in the gel state.

in the string-controlled regime and $(1 + 2c_s/c_p)^{-5/12}$ in the bead-controlled regime. The differences in the values of the exponent were used by Waigh et al.[22] to distinguish from string- to bead-controlled regimes of synthetic polyelectrolytes with quaternary ammonium moieties in various organic solvents at different ionic strengths. In this interpretation, the effect of the added salt concentration in chitosan solutions at DA = 2.7% and $c_p = 9.1$ g/L should reveal the string-controlled regime (see the log−log plots of $q_{max}(c_p)$ in Figures 3 and 4 with the scaling $q_{max} \sim c_p^{1/2}$). Figure 9 displays the evolution of the maximum of the polyelectrolyte peak with r_s, in a normalized scale with various added salts. As expected, the observed trend is in agreement with the theoretical predictions in the string-controlled regime.

For high DA values, we expect to find the bead-controlled regime if the nature of the anion is kept constant. When the anion is varied, for example, if sodium acetate is added to chitosan hydrochloride, an additional solvophilic effect should modify the value of q_{max} since, as discussed previously, the nature of the counterion affects the solvophobicity of the polymer−solvent pair in the case of chitosan.

From the Polyelectrolyte Solution to the Gel State. Chitosan physical hydrogels have received an immense and increasing interest owing to the diversity of their properties and their important applications in the biomedical field, for tissue engineering and tissue repair.[66,67] One of the keys to preserving the bioactive properties of chitosan solutions in the gel form is to avoid chemical modification of the polymer during hydrogel formation.

To obtain physical hydrogels, our strategy is to decrease the electrostatic interactions to enhance interchain hydrogen bonding and hydrophobic interactions when the initial polymer concentration is sufficiently high to ensure entanglements. Technically, two main routes were used. In the first, chitosan was dissolved in water by means of hydrochloric or acetic acid so as to achieve stoechiometric protonation of the NH_2 sites. After complete dissolution, an equivalent volume of 1,2-propanediol was added. The mixture was stirred and left to evaporate at 50 °C allowing a progressive elimination of water up to the gel point. These conditions yielded physical gels,[37] but as shown in Figure 10, a well-defined polyelectrolyte peak is still present, with an increase of the low-angle upturn even after long evaporation times.

As previously mentioned, evaporation of water decreases the dielectric constant of the medium by progressively leaving a less polar solvent. For DA close to 2.7%, the composition of the solvent thus evolves until the gel point is reached, when water is completely removed after an evaporation time close to 900 min. This results in a change of the effective charge fraction carried by the polyelectrolyte and a decrease of the ionic dissociation, then a reduction of the acidity of the hydrochloric acid in a medium where its solubility is also lower. Moreover, chitosan is more solvophobic in 1,2-propandiol than in water. With long evaporation times, the free hydrochloric acid present in the media can easily be eliminated.[37] This decreases the charge density of chitosan and favors solvophobic interactions and hydrogen bonding, thereby creating the physical junctions of the polymer network. This could explain why the scattering profile continues to evolve for longer times, particularly in the low q range. The polyelectrolyte peak is still visible after a large amount of evaporation has taken place, so that the alcoholic gels can be considered to be true polyelectrolyte gels. Unfortunately, it was not possible to obtain gels in monoalcohols such as methanol, ethanol, propanol, or butanol.[37] A first experimental explanation is that the boiling point of monoalcohols is too low as compared to water. They are also poorer solvents of chitosan than 1,2-propanediol. Second, for a particular balance between hydrophilic and hydrophobic parts in their structure, diols can also contribute to the formation of physical junctions by H-bonding.[35] The latter consideration was verified by using different diols.[37] Last, the gelation mechanism of these gels is reversible in the sense that addition of water to the gels again yields a solution.

In the second gelation route, the decrease of the charge density could be directly operated from a simple aqueous acidic solution of chitosan in contact with an alkaline gas such as ammonia.[36] The ammonia gas dissolves into the chitosan solution and contributes to the neutralization of amine functions in a slow and homogeneous way within the solution. This physicochemical perturbation occurs inside a thick layer, parallel to the surface of the initial solution, and constitutes a sol−gel transition interface moving from the top to the bottom of the reactor. Again, this results in a decrease of the charged monomer fraction of the polymer, which acts on the hydrophobic−electrostatic interaction balance, promoting interchain interactions by hydrophobic and H-bonds. The changes in the scattering curves during gelation of a chitosan solution (acetate counterions, DA = 46.2, c_p = 13.7 g/L) in contact with gaseous ammonia are shown in Figure 11.

In contrast to the gels obtained in 1,2-propanediol, the polyelectrolyte peak in these gels disappears fully at pH > 6.5, a finding that is simply explained by the neutralization of chitosan. Another feature of the scattering diagrams presented in Figure 11 is the presence of a fixed point, where all the

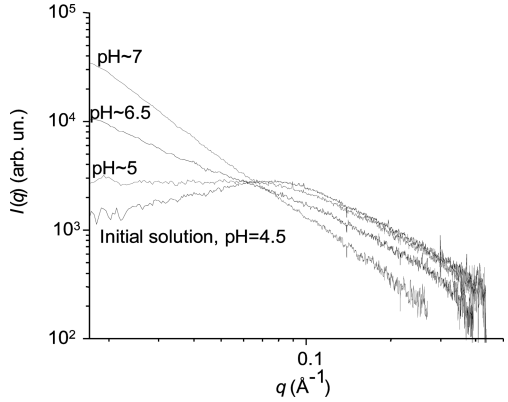

Figure 11. SAXS curves of chitosan acetate (DA = 46.2%, c_p = 13.7 g/L) as a function of the time of neutralization with ammonia and pH. On neutralization, the polyelectrolyte peak disappears, displaying an isobestic point.

intensities are independent of neutralization. Although the physical concepts behind this observation are not at present clear, this feature is not an isolated case and has been described as an isobestic point[4] in various polyelectrolyte DNA solutions with added salt.

In the characteristic size range of the screening length, the structure of the gels is thus sensitive to the gelation route, as gels obtained in 1,2-propanediol are different from those obtained by progressive neutralization.

Conclusion

Chitosan is a unique and versatile natural cationic polyelectrolyte that permits fundamental investigations on chain conformation and ordering in hydrophobic polyelectrolyte solutions under various experimental conditions. Our results can be explained and modeled in many aspects by invoking the theoretical work of Dobrynin and Rubinstein[1,62] and fully can explain the evolution of the polyelectrolyte correlation peak with concentration, the influence of the DA, and nature of the solvent. In particular, the study of the variation of q_{max} with c_p shows the existence of a transition of the necklace model from a structure controlled by the strings between pearls at low DAs (high charge density, $\alpha \sim 1/2$) to a situation dominated by the pearls at high DAs (low charge density, $\alpha \sim 1/3$). It is particularly noted that these results provide new arguments in favor of the general law of behavior[35,36,43,44,57] describing the variation of the physicochemical parameters of chitosan chains as a function of DA.

Between the two regimes, a crossover polymer concentration c_b is defined[62] and observed as the limit between the string- and the bead-controlled regimes. In previous papers on the formation mechanism of physical hydrogels of chitosan with no cross-linking agent,[35,36] a second critical concentration c^{**} was proposed, which was also conjectured to reflect the limit between two organizations of the initial solution. The present result confirms our previous hypotheses and provides a microscopic understanding of the molecular ordering of chitosan solutions at different concentrations.

For the first time, we show that the nature of the counterion influences the environment of cationic polymer chains. The hydrochloride form of chitosan is more solvophobic than that of the acetate, as a result of specific interaction mechanisms between chitosan and acetate counterions.

The formation of physical hydrogels of chitosan from either a hydro-alcoholic or an aqueous solution was also qualitatively investigated. The study of the polyelectrolyte peak in such systems yields understanding of the structural differences of chitosan gels as a function of the processing route. In the first case, the polyelectrolyte peak and the polyelectrolyte solution nanostructure is preserved, thus confirming the presence of charges in these kinds of gels, contrary to the second type of gels where NH_3^+ moieties progressively disappear with neutralization.

Acknowledgment. We thank Dr. I. Morfin and A. Crepet for their technical assistance and Dr. E. Geissler for his participation in improving the English language of the paper. We thank the ESRF and CRG groups for the SAXS experiments on the D2AM beamline. This work was funded by a grant from the Délégation Générale de l'Armement (DGA).

References and Notes

(1) Dobrynin, A. V.; Rubinstein, M. *Macromolecules* **2001**, *34*, 1964.
(2) Holm, C.; Kékicheff, P.; Podgornik, R. *NATO Sciences Series II Mathématics, Physics, and Chemistry*; Kluwer Academic: Dordrecht, The Netherlands, 2001; p 46.
(3) Skibinska, L.; Gapinski, J.; Liu, H.; Patkowski, A.; Fisher, E. W.; Pecora, R. *J. Chem. Phys.* **1999**, *110* (3), 1794.
(4) Borsali, R.; Nguyen, H.; Pecora R. *Macromolecules* **1998**, *31*, 1548.
(5) David, L.; Montembault, A.; Vizio-Boucard, N.; Crepet, A.; Viton, C.; Domard, A.; Morfin, I.; Rochas, C. *Macromol. Symp.* **2005**, *222* (1), 281.
(6) Mischenko, N.; Denef, B.; Koch, M. H. J.; Reyaners, H. *Int. J. Biol. Macromol.* **1996**, *19*, 185.
(7) Buhler, E.; Boue, F. *Eur. Phys. J. E* **2003**, *10*, 89.
(8) Xiang, W.; Tang, J. X.; Janmey, P. A.; Braulin, W. H. *Biochemistry* **1999**, *38*, 7219.
(9) Barrat, J. L.; Joanny, J. F. In *Advances in Chemical Physics, Polymeric Systems*; Progine, S. A., Ed.; John Wiley and Sons: New York, 1996; Vol. XCIV.
(10) Manning, G. S. *Biophys. Chem.* **1977**, *7*, 95.
(11) Manning, G. S. *Phys. A* **1996**, *231*, 236.
(12) De Gennes, P. G.; Pincus, P.; Velasco, R. M. *J. Phys. (Paris)* **1976**, *37*, 1461.
(13) Rubinstein, M.; Colby, R. H.; Dobrynin, A. V.; Joanny, J. F. *Macromolecules* **1996**, *29*, 398.
(14) Dobrynin, A. V.; Colby, R. H.; Rubinstein, M. *Macromolecules* **1995**, *28*, 1859.
(15) Wang, D.; Lal, J.; Moses, D.; Guillermo, C. B.; Heeger, A. J. *Chem. Phys. Lett.* **2001**, *38*, 411.
(16) Plestil, J. *Polymer* **1986**, *27*, 839.
(17) Essafi, W.; Lafuma, F.; Williams, C. E. *Eur. Phys. J. B* **1999**, *9*, 261.
(18) Essafi, W.; Lafuma, F.; Williams, C. E. *J. Phys. II* **1995**, *5*, 1269.
(19) Zhang, Y.; Douglas, J. F.; Ermi, B. D.; Amis, E. J. *J. Chem. Phys.* **2001**, *114* (7), 3299.
(20) Nishida, K.; Kaji, K.; Kanaya, T.; Shibano, T. *Macromolecules* **2002**, *35*, 4084.
(21) Nishida, K.; Kaji, K.; Kanaya, T. *Macromolecules* **1995**, *28*, 2472.
(22) Waigh, T. A.; Ober, R.; Williams, C. E.; Galin, J. C. *Macromolecules* **2001**, *34*, 1973.
(23) Tmosic, M.; Bester, R.; Jamnik, A. *Acta Chim. Slov.* **2001**, *48*, 333.
(24) Qu, D.; Baigl, D.; Williams, C. E.; Mohwald, H.; Fery A. *Macromolecules* **2003**, *36*, 6878.
(25) Baigl, D.; Ober, R.; Qu, D.; Fery, A.; Williams, C. E. *Europhys. Lett.* **2003**, *62* (4), 588.
(26) Knudsen, K. D.; Lauten, R. A.; Kjoniksen, A. L.; Nystrom, B. *Eur. Polym. J.* **2004**, *40*, 721.
(27) Yethiraj, A.; Shew, C. Y. *Phys. Rev. Lett.* **1996**, *77* (18), 3937.
(28) Stevens, M. J. *Phys. Rev. Lett.* **1999**, *82* (1), 101.
(29) Yethiraj, A. *Phys. Rev. Lett.* **1996**, *78* (19), 3789.
(30) Donley, J. P. *J. Chem. Phys.* **2002**, *116* (12), 5315.
(31) Anthonsen, M. W.; Varum, K. M.; Hermansson, A. M.; Smidsrod, O.; Brant, D. A. *Carbohydr. Polym.* **1994**, *25*, 13.
(32) Nishida, N.; Kaji, K.; Kanaya, T. *J. Chem. Phys.* **2001**, *115* (17), 8217.
(33) Roberts, G. A. F. McMillan Publishing: New York, 1992.
(34) Borzacchielollo, A.; Ambrosio, L.; Netti, P. A.; Nicolais, L.; Peniche, C.; Gallardo, A.; San Roman, J. *J. Mater. Sci.: Mater. Med.* **2001**, *12*, 861.

(35) Montembault, A.; Viton, C.; Domard, A. *Biomaterials* **2005**, 26 (8), 933.
(36) Montembault, A.; Viton, C.; Domard, A. *Biomacromolecules* **2005**, *6* (2), 653.
(37) Boucard, N.; Viton, C.; Domard, A. *Biomacromolecules* **2005**, *6* (6), 3227.
(38) Durera, H.; Tiwary, A. K.; Gupta, S. *Int. J. Pharm.* **2000**, *213*, 193.
(39) Banerjee, T.; Mitra, S.; Singh, A. K.; Sharma, R. K.; Maitra, A. *Int. J. Pharm.* **2002**, *243*, 93.
(40) Knaul, J. Z.; Hudson, S. M.; Creber, K. A. M. *J. Appl. Polym. Sci*. **1999**, *72*, 1721.
(41) Domard, A.; Domard, M. *Polymeric Biomaterials*, 2nd ed.; Severian Dumitriu: 2002; p 187.
(42) Sorlier, P.; Denuzière, A.; Viton, C.; Domard, A. *Biomacromolecules* **2001**, *2*, 765.
(43) Schatz, C.; Viton, C.; Delair, T.; Pichot, C.; Domard, A. *Biomacromolecules* **2003**, *4*, 641.
(44) Lamarque, G.; Lucas, J. M.; Viton, C.; Domard, A. *Biomacromolecules* **2005**, *6* (1), 131.
(45) Anthonsen, M. W.; Varum, K. M.; Smisdsrod, O. *Carbohydr. Polym.* **1993**, *22*, 193.
(46) Wang, W.; Bo, S.; Li, S.; Qin, W. *Int. J. Biol. Macromol.* **1991**, *13*, 281.
(47) Berth, G.; Dautzenberg, H. *Carbohydr. Polym.* **2002**, *47*, 39.
(48) Errington, N.; Harding, S. E.; Varum, K. M.; Illum, L. *Int. J. Biol. Macromol.* **1993**, *13*, 113.
(49) Berth, G.; Dautzenberg, H.; Peter Martin, G. *Carbohydr. Polym.* **1998**, *36*, 205.
(50) Berth, G.; Dautzenberg, H.; Peter Martin, G. *Carbohydr. Polym.* **1998**, *36*, 205.
(51) Buhler, E.; Rinaudo, M. *Macromolecules* **2000**, *33*, 2098.
(52) Colfen, H.; Berth, G.; Dautzenberg, H. *Carbohydr. Polym.* **2001**, *45*, 373.
(53) Wu, C.; Zhow, S.; Wang, W. *Biopolymers* **1995**, *135*, 385.
(54) Tsaih, M. L.; Chen, R. H. *Int. J. Biol. Macromol.* **1997**, *20*, 233.
(55) Anthonsen, M. W.; Varum, K. M.; Hermansson, A. M.; Smisdsrod, O.; Brant, D. A. *Carbohydr. Polym*. **1994**, *25*, 12.
(56) Lamarque, G.; Viton, C.; Domard, A. *Biomacromolecules* **2004**, *5*, 992.
(57) Sorlier P.; Viton, C.; Domard, A. *Biomacromolecules* **2002**, *3* (6), 1336.
(58) Terbojevich, M.; Carraro, C.; Cosani, A. *Carbohydr. Res.* **1988**, *180*, 73.
(59) Vachoud, L.; Zydowick, N.; Domard, A. *Carbohydr. Res.* **1997**, *302*, 169.
(60) Hirai, A.; Odani, H.; Nakajima, A. *Polym. Bull.* **1991**, *26*, 87.
(61) Sorlier, P.; Rochas, C.; Morfin, I.; Viton, C.; Domard, A. *Biomacromolecules* **2003**, *4*, 1034.
(62) Dobrynin, A. V.; Rubinstein, M. *Macromolecules* **1999**, *32*, 915.
(63) Terreux, R.; Domard, M.; Domard, A. *Adv. Chitin Sci.* **2006**, in press.
(64) Patkowski, A.; Gulari, E.; Chu, B. *J. Chem. Phys.* **1980**, *73*, 4178.
(65) Wang, L.; Bloomfield, V. A. *Macromolecules* **1991**, *24*, 5791.
(66) Mi, L. F.; Sung, H. W.; Shyu, S. S. *J. Polym. Sci.* **2000**, *38*, 2804.
(67) Montembault, A.; Tahiri, K.; Korwin-Zmijowska, C.; Corvol, M. T.; Domard, A. **2006**, *88*, 551.

BM060911M